

## Pressure-induced strong mode coupling and phase transitions in $\text{KNbO}_3$

Z. X. Shen and Z. P. Hu

*Department of Physics, National University of Singapore, Lower Kent Ridge Road, Singapore 0511*

T. C. Chong and C. Y. Beh

*Department of Electrical Engineering, National University of Singapore, Kent Ridge, Singapore 0511*

S. H. Tang and M. H. Kuok

*Department of Physics, National University of Singapore, Lower Kent Ridge Road, Singapore 0511*

(Received 9 March 1995)

Potassium niobate single-crystal samples have been studied by Raman scattering up to 200 kbar. The effect of pressure on  $\text{KNbO}_3$  is extremely large and there exists a rich variety of pressure-induced changes. Mode softening is found for some of the characteristic Raman bands of the orthorhombic phase. Intensity transfer and frequency repelling have been observed in the  $200\text{ cm}^{-1}$  region as a result of strong coupling between two  $B_1(\text{TO})$  modes, whose frequencies have been brought closer under pressure. There are three new crystalline phases and an amorphous phase in this pressure range, and two of the phase transitions are thought to be displacive type. The samples do not transform back to the ambient-pressure phase on decompression.

### INTRODUCTION

The barium titanate family ferroelectrics have outstanding electro-optical, nonlinear optical, photorefractive properties, and have found widespread applications in nonlinear optics and electro-optics. They are also the prototype perovskite ferroelectrics and their successive phase transformations provide the typical examples for the study of paraelectric and ferroelectric transitions. It is therefore not surprising that they have been among the most intensively studied materials. In particular,  $\text{BaTiO}_3$  provided a model substance for the original soft-phonon theory<sup>1</sup> and the theory of ferroelectrics.<sup>2</sup> The properties of potassium niobate ( $\text{KNbO}_3$ ) are similar to that of barium titanate and have been studied by many techniques.<sup>3–10</sup>  $\text{KNbO}_3$  shows four solid phases—one paraelectric and three ferroelectric at variable temperature.<sup>5,11–14</sup> On cooling, the following phase transitions are found: cubic ( $C$ ) to tetragonal ( $T$ ) at 701 K, tetragonal to orthorhombic ( $O$ ) at 488 K and finally to rhombohedral ( $R$ ) at 210 K.<sup>5</sup> In the high-temperature  $C$  phase,  $\text{KNbO}_3$  is paraelectric. When the crystal is cooled below the phase transition temperature 701 K, spontaneous polarization develops along the  $c$  axis, so that the  $c$  direction becomes nonequivalent with the other two and the crystal undergoes a phase transformation to the ferroelectric  $T$  phase. As the temperature is lowered further, the successive phase transitions to the ferroelectric  $O$  and  $R$  phases involve the polarization direction changes to face diagonal and body diagonal, respectively.<sup>12</sup>  $\text{KNbO}_3$  provides a very good example for the study of the nature of structural phase transitions. Much of the work on  $\text{KNbO}_3$  have been to study the mechanisms of these transitions, as to whether they are displacive characterized by a soft mode, or order-disorder charac-

terized by a central peak.<sup>5–7,9,14–18</sup> While the softening of a transverse optical mode above each transition favors a displacive model for the transitions, disorder-order-type transitions for the  $C$ - $T$  and  $T$ - $O$  phase transitions have also been proposed. Raman spectroscopy has been particularly widely used in these studies.

Besides temperature variation, pressure change is another useful variable which provides complementary information to the variable temperature data. But it has been largely neglected in the study of physical properties and mechanisms in the past mainly because the relative difficulties involved in the generation of high pressure and the coupling of high-pressure apparatus to the experiments. With the wide use of the diamond-anvil high-pressure cell in the recent years, high-pressure data have become quite common especially in the field of spectroscopy. A number of the barium titanate family ferroelectrics have been studied under high pressure, e.g.,  $\text{BaTiO}_3$ ,<sup>19,20</sup>  $\text{LiNbO}_3$ ,<sup>21–23</sup> and  $\text{LiTaO}_3$ .<sup>22,23</sup> But to the best of our knowledge, no high-pressure experiment has been performed on  $\text{KNbO}_3$ .

### EXPERIMENT

$\text{KNbO}_3$  crystal samples used in the experiment were grown from melt comprised of a mixture of  $\text{K}_2\text{CO}_3$  and  $\text{Nb}_2\text{O}_5$  using the top-seeded solution growth technique, the details of which will be described elsewhere. High pressure was generated by a gasketed diamond-anvil cell. The stainless steel gaskets used are  $200\text{ }\mu\text{m}$  in thickness with a hole of  $200\text{ }\mu\text{m}$  in diameter. The gaskets are preindented before samples were loaded. A small crystal sample and a ruby chip were loaded into the gasket hole together with 4:1 mixture of methanol-ethanol, which acts as quasihydrostatic pressure transmitting medium.

The pressure was calibrated by the ruby fluorescence technique.<sup>24</sup> Raman spectra were recorded in the back-scattering geometry using a Spex double monochromator coupled to a conventional photon counting system. The 488 nm line of an Ar<sup>+</sup> ion laser was used as the excitation source. All high-pressure spectra were taken at room temperature. Although single-crystal samples were used in our experiments no particular care was taken to align the samples, so that the Raman peaks recorded were made up of all allowed symmetries.

## RESULTS

The structures of KNbO<sub>3</sub> in different ambient pressure phases have been studied by Hewat<sup>13</sup> by neutron diffraction. The ambient condition orthorhombic phase belongs to space group  $C_{2v}^{14}(Amm2)$ , with 1 formula group in the unit cell. The 12 optical modes in the  $C_{2v}$  point group are:  $4A_1 + 4B_1 + 3B_2 + A_2$ . All the modes are Raman active, and all the modes except the  $A_2$  mode are also infrared IR active. Polarized Raman spectra have been recorded (see for example Ref. 3) and all of expected Raman bands have been identified, including the bands due to the splitting of the TO and LO modes. Since the Raman spectra recorded are unpolarized in our high-pressure experiment, peaks of all symmetry species are collected the same time. Fewer peaks are observed due to the overlapping and mixing of the modes.

Figures 1(a) and 1(b) shows the Raman spectra of KNbO<sub>3</sub> at different pressures and the observed Raman bands are listed in Table I. The peaks obtained from the polarized Raman spectra by Quittet *et al.*<sup>3</sup> are also given in Table I. It can be seen that the two results agree reasonably well. There exists a strong continuous background in the spectrum,<sup>3,5</sup> which makes it difficult to determine the frequencies of some low-frequency bands. This may explain the 11 cm<sup>-1</sup> difference for the band at 51 cm<sup>-1</sup> between our result and that of Ref. 3. In fact, Fontana *et al.*<sup>5</sup> and Bozinis and Hurrell<sup>4</sup> have reported the same band at 50 and 56 cm<sup>-1</sup>, respectively, closer to our result. There is a dip on the low-frequency side of the sharp 196 cm<sup>-1</sup> band. This has been explained as an interference between this band and the continuous background<sup>3</sup> using a model developed by Fano.<sup>25</sup> In the 280 cm<sup>-1</sup> region, we can clearly identify three peaks at ambient pressure, which would consist of a broad peak at 266 cm<sup>-1</sup>, another broad peak at 280 cm<sup>-1</sup> and a sharp peak at 298 cm<sup>-1</sup> (see spectrum *a* in Fig. 1). But from the spectra at higher pressure in Fig. 1, a sharp peak clearly exists at about 280 cm<sup>-1</sup>. We therefore identified four bands in this region. The peak frequency for the 266 cm<sup>-1</sup> band may be overestimated in our case as it is overlapping with another broad band at higher frequency. For the same reason, the frequency of the 51 cm<sup>-1</sup> peak may have been underestimated.

In Figs. 2 and 3, the pressure dependence of the Raman frequencies are plotted. As the pressure is increased, the frequency of the band at 50 cm<sup>-1</sup> decreases and disappears into the increasing background of the continuum at about 20 kbar (spectra *b* and *c* in Fig. 1). The band at 266 cm<sup>-1</sup>, which appears as a shoulder at ambient

pressure gains strength with pressure while its frequency softens. The intensity of the broad band at 280 cm<sup>-1</sup> decreases drastically with pressure and it has almost disappeared by 13 kbar, so that the 266 cm<sup>-1</sup> band becomes nearly symmetrical with two very sharp bands on its high-frequency shoulder at 282 and 296 cm<sup>-1</sup>, respectively. The presence of these two bands becomes more evident with increasing pressure as they are separated more and more from the broad bands because the diminishing

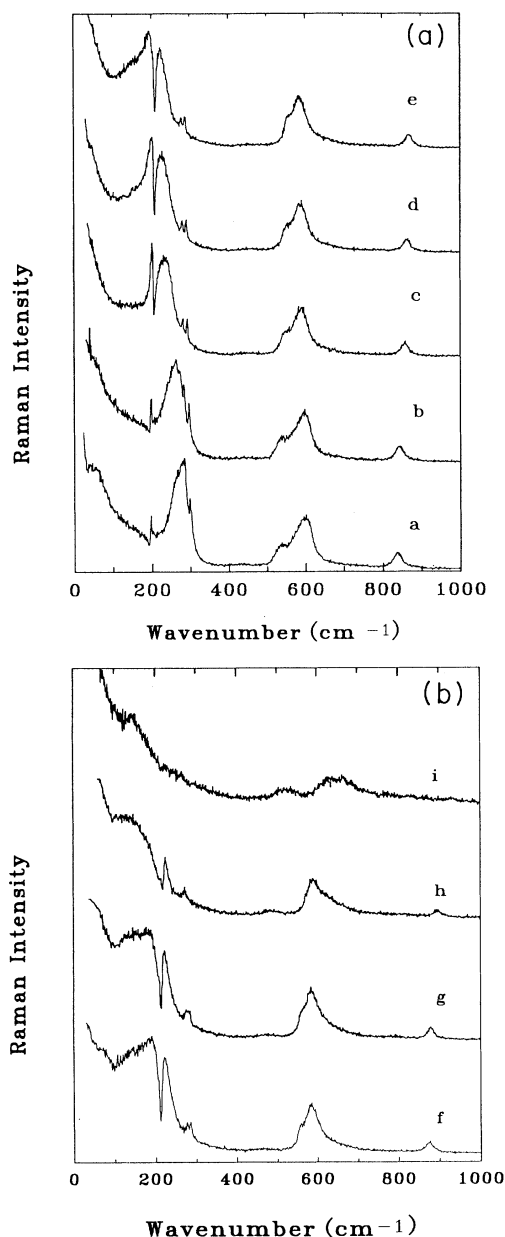


FIG. 1. (a) The high-pressure Raman spectra of KNbO<sub>3</sub> in the pressure increase sequence. Spectrum *a*: 2.4 (O phase), *b*: 10.4 (O), *c*: 35.7 (HPI), *d*: 47.7 (HPI), and *e*: 58.3 kbar (HPI). (b) The high-pressure Raman spectra of KNbO<sub>3</sub> in the pressure increase sequence. Spectrum *f*: 68.2 (HP11), *g*: 77.9 (HP11), *h*: 109 (HP11), and *i*: 186 kbar (amorphous).

TABLE I. The observed Raman band frequencies and assignments (in comparison with Ref. 3) of  $\text{KNbO}_3$  at ambient pressure.

Freq./ $\text{cm}^{-1}$ (Ref. 3)	Assignment (Ref. 3)	Freq./ $\text{cm}^{-1}$	Assignment
40(27×2) <sup>a</sup>	$B_2(\text{TO})$	51	$B_2(\text{TO})$
192(2)	$B_1(\text{TO})$		
193(2)	$A_1(\text{TO})$	196	Mixed
194.5(3)	$A_1(\text{LO})$		
196.5	$B_2(\text{TO})$		
249(25)	$B_1(\text{TO})$		
270	$B_1(\text{TO})$	266( <i>s,br</i> )	$B_1(\text{TO})$
281.5(33)	$A_1(\text{TO})$	280( <i>s,br</i> )	$A_1(\text{TO})$
282(6)	$A_2$	283( <i>sp</i> )	$A_2$
295(5)	$A_1(\text{LO})$		
297(5)	$A_1(\text{TO})$	298( <i>sp</i> )	$A_1(\text{LO}) + A_1(\text{TO})$
434.5(10)	$A_1(\text{LO})$	435( <i>uv,br</i> )	$A_1(\text{LO})$
513(20)	$B_2(\text{TO})$		
534(20)	$B_1(\text{TO})$	535( <i>m,br</i> )	$B_1(\text{TO})$
606.5(33)	$A_1(\text{TO})$	597( <i>s,br</i> )	$A_1(\text{TO})$
834(27)	$A_1(\text{LO})$	836( <i>m,br</i> )	$A_1(\text{LO})$

<sup>a</sup>The figure in parentheses is the full width at half maximum in wave number.

of the 280  $\text{cm}^{-1}$  band and the softening of the 266  $\text{cm}^{-1}$  band. The two bands themselves and the one at 597  $\text{cm}^{-1}$  also soften slightly with compression. The broad band at 435  $\text{cm}^{-1}$  is barely seen below 80 kbar, but above which pressure its intensity increases steadily. The other bands show the expected strengthening in the 0–20 kbar range.

In the 20–40 kbar range, the soft mode at 50  $\text{cm}^{-1}$  has

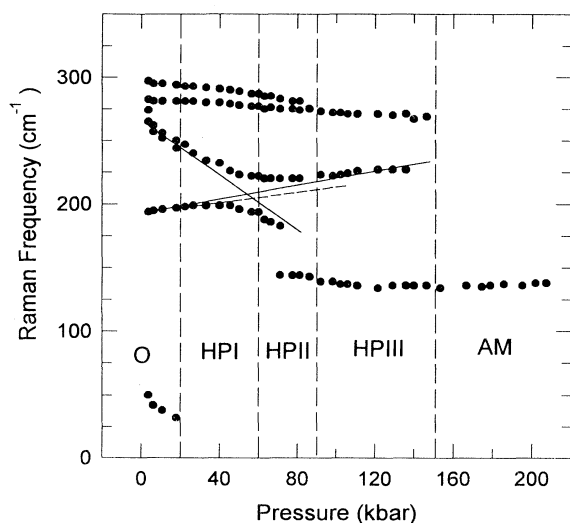


FIG. 2. The pressure dependence of the Raman frequencies for the bands below 300  $\text{cm}^{-1}$ . The vertical dashed lines indicate the proposed phase transition pressures. The two solid lines act as guide for the two  $B_1(\text{TO})$  modes if no coupling were present, while the dotted line represents the pressure dependence of the frequency for the very weak sharp band not involved in the coupling.

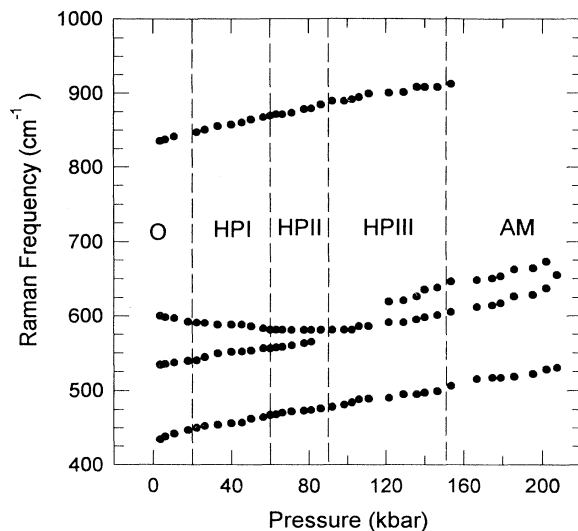


FIG. 3. The pressure dependence of the Raman frequencies for the bands above 300  $\text{cm}^{-1}$ . The vertical dashed lines indicate the proposed phase transition pressures.

disappeared. The band at 196  $\text{cm}^{-1}$  shows the most dramatic changes in this pressure range. Its intensity is about constant below 20 kbar, however it increases drastically with pressure and it also broadens considerably. Furthermore, the dip originally at the low-frequency side has now changed to the high-frequency side. The 266  $\text{cm}^{-1}$  band continues to soften and its width narrows slightly.

When the sample was further compressed to the 40–50 kbar range, the broadening of the 196  $\text{cm}^{-1}$  band accelerates and the 266  $\text{cm}^{-1}$  band narrows fast. At the same time, both bands become very asymmetric. Above 50 kbar, the low-frequency band becomes broader than the high-frequency band. Hence the trend looks to be the reverse of that for the low-pressure region. We suggest that there is a cross over of these two bands at about 50 kbar, so that the high-frequency peak carries the characteristics of the low-frequency one and vice versa above this pressure. The asymmetrical shape of the high-frequency band remains at least to 100 kbar. There seems to be a very weak sharp band at the 200  $\text{cm}^{-1}$  region whose frequency increases linearly with pressure. This band does not show clearly for spectra presented in Fig. 1 but becomes more evident for experiments performed with bigger samples.

At about 60 kbar a new band develops at about 150  $\text{cm}^{-1}$ . Its intensity increases with pressure at the expense of the broad peak at 200  $\text{cm}^{-1}$ , while the frequency remains roughly constant. Its apparent intensity (not corrected for the continuous background) matches that of the 200  $\text{cm}^{-1}$  peak at 85 kbar and the latter gradually disappears into the background at about 100 kbar.

At 90 kbar, several spectral changes were observed: (1) The two sharp peaks at the 300  $\text{cm}^{-1}$  region converge and merge into a single band. (2) The two peaks originally at 597 and 535  $\text{cm}^{-1}$  cross over because the softening of the former and the stiffening of the latter. The frequencies of both bands increase with further compression.

sion. It is remarkable that the merge of the bands at the  $300\text{ cm}^{-1}$  region occurs at the same pressure as the crossover of the  $500\text{ cm}^{-1}$  region bands. At higher pressures, all the sharp bands become weaker and cannot be detected above 150 kbar. There are only four broad bands left at 138, 518, 626, and  $662\text{ cm}^{-1}$ , respectively.

The Raman spectra on decompression are shown in Fig. 4. They are similar to those in the pressure increase sequence, so that the pressure effects are largely reversible. But at low pressure, the sample does not transform back to the ambient pressure phase, as demonstrated by the absence of the low-frequency soft mode. The continuous background and the signal-to-noise ratio for the pressure-released spectrum are comparable to that for the virgin spectrum. So that the missing soft mode cannot be explained by increased background noise. In addition, the dip on the  $200\text{ cm}^{-1}$  peak is on the high-frequency side, which also resembles spectrum *c* [belonging to a high-pressure phase (PHI)] rather than spectra *a* and *b* (belonging to the *O* phase) in Fig. 1.

#### DISCUSSION

The successive phase transitions of  $\text{KNbO}_3$  with temperature have been the subject of intense studies by many techniques. Although the low-frequency band at  $50\text{ cm}^{-1}$  is found to soften through all the phase transitions *C-T-O-R*, only the *O-R* transition is thought to be displacive originated by this soft mode. The other two transitions, including the paraelectric to ferroelectric *C-T* transition, are considered as order-disorder type, which can be explained by a eight-site model.<sup>15,9</sup> In our high-pressure study, the  $50\text{ cm}^{-1}$  mode is also found to be a soft mode, which disappears at about 20 kbar. In the 0–20 kbar range, the broad peak at  $280\text{ cm}^{-1}$  also disappears, which may show more clearly if polarized Raman

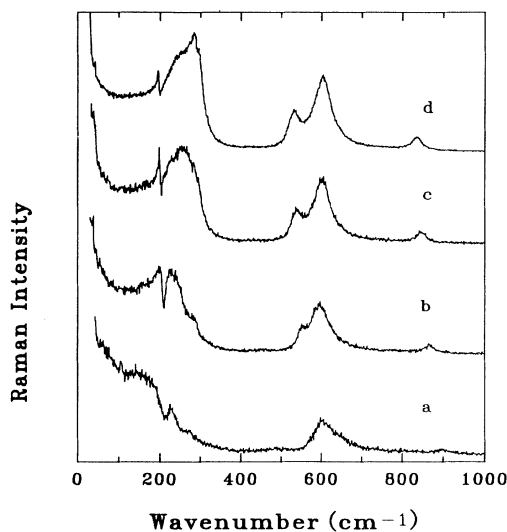


FIG. 4. The high-pressure Raman spectra of  $\text{KNbO}_3$  in the pressure decrease sequence. Note the soft mode at  $50\text{ cm}^{-1}$  is missing in the pressure released spectrum. Spectrum *a*: 126, *b*: 58, *c*: 22 kbar, and *d*: 1 bar (pressure released).

spectra are taken. We propose a displacive type phase transition at 20 kbar.

In the high-pressure phase, which we shall call high-pressure phase I (HPI), the asymmetric shape of the  $200\text{ cm}^{-1}$  peak is reversed. This is a manifestation of the coupling between this broad  $B_1(\text{TO})$  mode and the  $B_1(\text{TO})$  component of the peak at  $200\text{ cm}^{-1}$ . This coupling becomes stronger as the two peaks get closer because of the softening of the high-frequency peak and the strengthening of the low-frequency peak. As a result of the coupling, some intensity of the strong peak is transferred to the weaker one. At the crossover point at about 50 kbar, the coupling effect reaches a maximum and consequently the two bands look very different from the uncoupled ones. On further compression, the two bands move away from each other and their respective band shapes are gradually restored. The solid lines in Fig. 2 give a guide to the pressure dependence of the two bands if coupling did not exist. The frequencies of the two bands deviate more from the lines near the crossover point as the coupling effect is to make the two bands repel each other. There is a weak band in this region and its frequency is marked by the dotted line in Fig. 2. We suggest that it is another component of the  $200\text{ cm}^{-1}$  band of symmetry different from  $B_1(\text{TO})$ . This band is not expected to couple with the broad band, and its frequency increases linearly with pressure as a result. We see this as an additional support for our crossover discussion here.

There is another phase transition (from HPI to HPII) at 60 kbar, as indicated by the broad new low-frequency band at  $150\text{ cm}^{-1}$ . The intensity of this band increases at the expense of the soft mode at  $190\text{ cm}^{-1}$ . The merging of the two sharp bands in the  $300\text{ cm}^{-1}$  region and the crossover of the two bands in the  $600\text{ cm}^{-1}$  region demonstrate another phase transition (HPII/HPIII) at 90 kbar. It is noteworthy that the extrapolation of the soft mode at  $190\text{ cm}^{-1}$  will also meet the  $150\text{ cm}^{-1}$  peak at the same pressure, so that this phase transition may also be a displacive type. As phase HPIII has fewer bands, we believe that it possesses a higher symmetry than the lower pressure phases. The sample may be amorphous above 150 kbar as all the bands are very broad. On decompression, the soft mode is missing and the dip for the  $200\text{ cm}^{-1}$  peak is on the high-frequency side, therefore the sample may not go back to the ambient pressure phase, but instead remains in the HPI phase.

The pressure effects on the  $\text{ABO}_3$ -type perovskite ferroelectrics have been studied by several authors by spectroscopic method.<sup>20,22,23,26–28</sup> No soft modes have been found for  $\text{LiNbO}_3$  and  $\text{LiTaO}_3$ .<sup>22,23</sup> In the high-pressure Raman study of  $\text{PbTiO}_3$  (Refs. 26–28) and  $\text{BaTiO}_3$ ,<sup>28</sup> soft modes obeying the Curie-Weiss-type law  $\omega \propto (P - P_0)^{1/2}$  have been observed. In the case of  $\text{PbTiO}_3$ , the phase transition at  $\sim 100$  kbar is believed to be the same ferroelectric (*T*) to the paraelectric (*C*) phase transition observed at 765 K under ambient pressure. The *T* phase has a larger unit-cell volume than the *C* phase, the application of pressure therefore favors the cubic phase, reducing the Curie temperature  $T_C$  and making the transition possible at room temperature. In Raman experi-

ments, the intensities of all the Raman bands decrease sharply on approaching the transition pressure as there are no first-order Raman-active bands in the *C* phase. The ferroelectric to paraelectric phase transition for BaTiO<sub>3</sub> occurs at a very modest 19 kbar.<sup>28</sup>

In comparison with PbTiO<sub>3</sub> and BaTiO<sub>3</sub>, one natural question to ask for KNbO<sub>3</sub> would be: is any of the high-pressure phases the same as the phases obtainable by temperature variation? Like in PbTiO<sub>3</sub>, there are also no Raman-active bands in the *C* phase for KNbO<sub>3</sub>, however quite strong Raman bands have been observed for all the phases in our experiments up to 200 kbar. So that none of the high-pressure phases is the paraelectric cubic phase. Another high-temperature phase for KNbO<sub>3</sub> is the ferroelectric *T* phase. The lattice parameters in this phase is considerably larger than that of the orthorhombic phase, so that the *T* phase is less dense than the *O* phase.<sup>11</sup> It is therefore unlikely that the ambient pressure *T* phase can be obtained by compression. The last ambient pressure phase is the low-temperature *R* phase. Although the *O*-*R* transition at 210 K is also characterized by this soft mode at 50 cm<sup>-1</sup> like the *O*-PHI transition at 20 kbar, the strong continuous background disappears completely in the *R* phase, whereas it is just as strong in the PHI phase. Moreover, the Raman bands at 266 and 600 cm<sup>-1</sup> continue to soften after the *O*-PHI transition, where the rate of the former is quite large. But they do not show any softening behavior in the low-temperature phase with cooling, which is analogous to pressure due to thermal contraction. We therefore suggest that the two

phases are different. Hence we conclude that all the high-pressure phases found are new phases.

### CONCLUSIONS

Based on the results and discussion presented above, we conclude the following:

(i) A displacive type phase transition has been found at 20 kbar. This transition is mainly characterized by the low-frequency soft mode.

(ii) In the HPI phase stable region between 20–60 kbar, very strong mode coupling occurs between the two *B*<sub>1</sub>(TO) bands, one being the very sharp band at 196 cm<sup>-1</sup> and a broad soft mode at 266 cm<sup>-1</sup>. The coupling is the strongest at the crossover pressure at 50 kbar.

(iii) A phase transition occurs at 60 kbar. It is indicated by the new broad band at 150 cm<sup>-1</sup>. Its frequency is nearly independent of pressure.

(iv) The phase transition at 90 kbar is displacive characterized by the soft mode with ambient frequency 266 cm<sup>-1</sup>. The symmetry of this phase (HPIII) should be higher than the other phases since it has fewer Raman bands.

(v) The phase above 150 kbar may be amorphous as all the bands are broad.

(vi) On decompression, the sample is reversible by large. However it does not revert back to the ambient pressure phase, but remains in the HPI phase.

(vii) All the phases found are high-pressure phases. They cannot be obtained by varying temperature at ambient pressure.

<sup>1</sup>W. Cochran, *Adv. Phys.* **9**, 387 (1960).

<sup>2</sup>A. F. Devonshire, *Adv. Phys.* **3**, 85 (1954).

<sup>3</sup>A. M. Quittet, M. I. Bell, M. Krauzman, and P. M. Raccah, *Phys. Rev. B* **14**, 5068 (1976).

<sup>4</sup>D. G. Bozinis and J. P. Hurrell, *Phys. Rev. B* **13**, 3109 (1976).

<sup>5</sup>M. D. Fontana, G. Metrat, J. L. Servoin, and F. Gervais, *J. Phys. C* **16**, 483 (1984).

<sup>6</sup>M. D. Fontana, A. Ridah, G. E. Kugel, and C. Carabatos-Nedelec, *J. Phys. C* **21**, 5853 (1988).

<sup>7</sup>R. Currat, R. Comes, B. Dorner, and E. Wiesendanger, *J. Phys. C* **7**, 2521 (1974).

<sup>8</sup>J. Hulliger, R. Gutmann, and H. Wuest, *J. Crystal Growth* **128**, 897 (1992).

<sup>9</sup>T. P. Dougherty, G. P. Wiederrecht, K. A. Nelson, M. H. Garrett, H. P. Jensen, and C. Warde, *Science* **258**, 770 (1992).

<sup>10</sup>M. D. Fontana, G. Dolling, G. E. Kugel, and C. Carabatos, *Phys. Rev. B* **20**, 3950 (1979).

<sup>11</sup>G. Shirane, H. Danner, A. Pavlovic, and R. Pepinsky, *Phys. Rev.* **93**, 672 (1954).

<sup>12</sup>R. Comes, M. Lambert, and A. Guinier, *Acta Crystallogr. A* **26**, 244 (1970).

<sup>13</sup>A. W. Hewat, *J. Phys. C* **6**, 2559 (1973).

<sup>14</sup>S. L. Chaplot and K. R. Rao, *J. Phys. C* **16**, 3045 (1983).

<sup>15</sup>Y. Luspin, J. L. Servoin, and F. Gervais, *J. Phys. C* **13**, 3761 (1980).

<sup>16</sup>R. Comes, M. Lambert, and A. Guinier, *Solid State Commun.* **6**, 715 (1968).

<sup>17</sup>J. P. Sokoloff, L. L. Chase, and D. Rytz, *Phys. Rev. B* **38**, 597 (1988).

<sup>18</sup>T. P. Dougherty, G. P. Wiederrecht, K. A. Nelson, M. H. Garrett, H. P. Jenssen, and C. Warde, *Phys. Rev. B* **50**, 8996 (1994).

<sup>19</sup>Y. Akishige, H. Takahashi, N. Mori, and E. Sawaguchi, *J. Phys. Soc. Jpn.* **63**, 1590 (1994).

<sup>20</sup>Y. Akishige, J. Nakahara, and E. Sawaguchi, *J. Phys. Soc. Jpn.* **60**, 1115 (1991).

<sup>21</sup>J. A. H. da Jornada, S. Block, F. A. Mauer, and G. J. Piermarini, *J. Appl. Phys.* **57**, 842 (1985).

<sup>22</sup>J. Mendes-Filho, V. Lemos, and F. Cerdeira, *J. Raman Spectrosc.* **15**, 367 (1984).

<sup>23</sup>A. Jayaraman and A. A. Ballman, *J. Appl. Phys.* **60**, 1208 (1986).

<sup>24</sup>J. D. Barnett, S. Block, and G. J. Piermarini, *Rev. Sci. Instrum.* **44**, 1 (1973).

<sup>25</sup>U. Fano, *Phys. Rev.* **124**, 1866 (1961).

<sup>26</sup>F. Cerdeira, W. B. Holzapfel, and D. Bauerle, *Phys. Rev. B* **11**, 1188 (1975).

<sup>27</sup>J. A. Sanjurjo, E. Lopez-Cruz, and G. Burns, *Solid State Commun.* **48**, 221 (1983).

<sup>28</sup>A. Jayaraman, J. P. Remeika, and R. S. Katiyar, in *High Pressure in Science and Technology*, edited by C. Homan, R. K. MacCrone, and E. Whalley, MRS Symposia Proceedings No. 22 (Materials Research Society, Pittsburgh, 1984), Pt. 1, pp. 165–168.